SURFACE WAVE MODELLING AND SIMULATION FOR WAVE TANKS AND COASTAL AREAS

E. (Brenny) van Groesen, University of Twente NL, and LabMah-Indonesia, Bandung RI
T. Bunnik, Maritime Research Institute Netherlands, Wageningen, NL
Andonowati, Bandung Institute of Technology, Bandung RI, and LabMath-Indonesia, Bandung RI

SUMMARY

For testing ships and offshore structures in hydrodynamic laboratories, the sea and ocean states should be represented as realistic as possible in the wave tanks in which the scaled experiments are executed. To support efficient testing, accurate software that determines and translates the required wave maker motion into the downstream waves is very helpful. This paper describes an efficient hybrid spatial-spectral code that can deal with simulations above flat and varying bottom. The accuracy of the code will be illustrated by presenting comparisons of simulations with experimental data for various different type of non-breaking waves, from dispersive focussing waves to irregular wave fields with freak waves; the very broad-band spectra of such waves provide the main challenge.

NOMENCLATURE

[Symbol]	[Definition] [(unit)]
η	Surface elevation (m)
ω	Frequency (rad s^{-1})
Ω	Dispersion relation (rad s^{-1})
f	Frequency (s^{-1})
k	wave number (rad m^{-1})
g	Gravitational acceleration (m s^{-2})
x	spatial coordinate (m)
t	time (s)

1. INTRODUCTION

The efficiency of wave tank operations is very much determined by the possibility to simulate accurately beforehand the waves that result from a given wave maker motion. Or, conversely, to determine the wave maker motion from an inverse simulation of a desired wave field at a specified position in the wave tank. In this contribution we describe a wave model and its implementation that can perform the task to calculate the surface elevation in the tank that results when the time signal of the elevation is given at a specific position. Using a linear or nonlinear transfer method that relates the wave maker motion and the surface elevation at the wave maker position, the main aim can then be achieved.
Characteristic for the dynamics of waves in the coastal area are the interplay of different physical effects, namely dispersion, nonlinearity and effects of bathymetry. For irregular, wind generated waves the spectra are broad; this naturally leads to high requirements to model the dispersion correctly over a large interval of wave lengths. But even for rather narrow-banded wave spectra, nonlinear effects can lead to short waves of double or triple the peak frequency that contribute to the wave heights of large waves. The calculation of long waves by nonlinear and bathymetric effects is important, for instance to detect waves that have frequencies for which ships, such as moored LNG-carriers, are resonant (typically 50-150 seconds).

To show the performance of the AB-wave model introduced by Van Groesen & Andonowati [1] and its implementation that will be described in Section 2, we will compare simulations with well recorded experiments performed at MARIN. In Section 3 details of the measurements are given. In section 4 we will compare simulations and measurements of four different wave cases. The first case is a well-designed focussing wave group above flat bottom, which test both the dispersive quality over a broad range of wave lengths, as well as nonlinear short wave generation in a narrow area near the focussing point. The second case above flat bottom is the well-known Draupner wave, one of very few recorded freak wave in natural surroundings. Two other cases concern waves running from deep to shallower depth via a straight slope; a bi-chromatic wave shows substantial short and long wave generation, while an irregular wave shows freak-like waves. In the conclusion section we comment on various related topics.

2. WAVE MODEL AND IMPLEMENTATION

In this section we describe the basics of the wave model and after that the hybrid spatial-spectral implementation.

2.1 VARIATIONAL WAVE MODELLING

Classical Mechanics deals with dynamical systems with a finite number of degrees of freedom and shows that when friction is absent, the equations can be formulated in canonical ways as a Lagrangian or Hamiltonian system. Characteristic is that such systems are solely determined by the total energy, and that such systems can be derived from a variational principle, the Lagrangian or action principle. Remarkably, the same holds true for surface waves on a layer of inviscid fluid, when the motion is restricted to irrotational flows. This basic property follows from Luke's variational principle [2], and the Hamiltonian structure was described by Zakhorov [3]; see also Broer [4] and Miles [5]. It turns out that this fundamental property can be used in a practical way for the design of wave models, by approximating the total energy to various degrees of accuracy. This is detailed

for uni-directional waves in the first subsection; a practical implementation described in the second subsection will respect this basic structure.

2.1 (a) The AB-model for waves above flat bottom

The Hamiltonian structure mentioned above requires to write the total energy as an expression in the surface elevation $\eta=\eta(x,t)$ and the fluid potential at the surface. To approximate the kinetic energy, which is the energy of the internal fluid motion, it turns out to be easier to use the fluid potential at the still water level. Then for small amplitude waves in the linear theory the energy can be found explicitly using Airy theory. In [1], a further restriction to uni-directional waves was imposed by relating the still water level potential to the surface elevation in the linear approximation. The governing equation then becomes a first order equation in the elevation only, and is of the form

(1) $\partial_t \eta = -A\, \delta H(\eta)$

where $\partial_t \eta$ denotes the partial time derivative, and $\delta H(\eta)$ is the variational derivative of the functional H. This functional is the approximate total energy, the Hamiltonian, and is given by

(2) $H(\eta)=1/(2) \int [\, \eta^2+\eta \,\{g(B\eta)^2-(A\eta)^2 /g\}/2 \,]\, dx$

The first term under the integral sign is the sum of the potential energy and the kinetic energy of the linear evolution. The other two terms are nonlinear contributions of second order; the terms in curly bracket are the difference of the squares of the horizontal and vertical velocity at the still water level. The linearized equation (1) reads $\partial_t \eta = -A\, \eta$.

A and B are (pseudo-) differential operators, related by $AB = \partial_x$. Explicitly, the operator A is skew symmetric and its action on a spatial function η is defined after Fourier transform as a multiplication with $i\Omega$:

(3) $A\, \eta(x) = \int i\, \Omega(k,D)\, \eta(k)\, e^{ikx}\, dk$

Here Ω denotes the dispersion relation $\omega=\Omega(k,D)$ such that the harmonic mode $exp\ i(kx - \Omega t)$ is a solution of the linear equation. For exact dispersion,

(4) $\Omega_{ex}(k,D)$= sign(k). sqrt $(g\, k$ tanh $(kD))$

where D is the depth. Exact dispersion describes the correct linear evolution of modes of *any* wave length. Approximate dispersion relations, for instance rational approximations of (4) that can be implemented in finite difference or finite elements, will give deviations in phase speed related to the difference with (4). The operator B is the inverse of the phase velocity.

The cubic terms in the Hamiltonian lead to dispersive correct quadratic terms in the equation (1).

2.1 (b) Generalization to waves above bathymetry

Waves travelling above varying bottom will have different phase and group speed depending on the depth at the actual position. For rather slowly varying bottoms, this motivates the use of a quasi-homogeneous approximation, in which the dispersion relation is taken locally. In the expression (3) for the operator A, for instance, this would mean to change the depth D by the space dependent function $D(x)$. However, in order not to violate the variational structure behind the equation (1), we need to replace the operator A by its skew-symmetric part, and similarly the operator B by its symmetric part. More details can be found in Van Groesen & Andonowati [7].

2.2 SPATIAL-SPECTRAL IMPLEMENTATION

As stated in the introduction, for broadband spectra it is essential that the dispersion is sufficiently accurate. For long waves (the shallow water limit) the relation is linear while for short waves (deep water) it is a square root relation. Finite difference, finite elements or volume of fluid methods cannot deal with non-rational relations, which therefore require approximations of the dispersion. By using a hybrid spatial-spectral code, problems with approximating the dispersion can be avoided. Indeed, for the equation Fourier transformed from physical to wavenumber space, the operator A in (3) can be applied exactly, so that the phase speed is accurate for all wave lengths. As is common in pseudo-spectral methods, products in physical space are calculated in physical space using back and forth fast Fourier transforms.

In case of varying bottom, an application of the operator A would require n^2 fast Fourier transforms. To reduce this to order n transforms, we interpolated the dispersion relation between the extreme values of the depth, requiring the frequency and phase speed to be exact at the peak frequency. Full details of the implementation will become available in [8].

3. EXPERIMENTS

3.1 BASIN

The experiments where all carried out in MARIN's shallow water basin, which has a length of 220 m, a width of 15.8 m and a maximum water depth of 1.1 m. The water depth can be controlled by pumping in or out water. The basin is equipped with a piston-type wave maker on the short side, controlled with a second-order control algorithm. On the opposite short side, a beach is installed to minimize wave reflections.

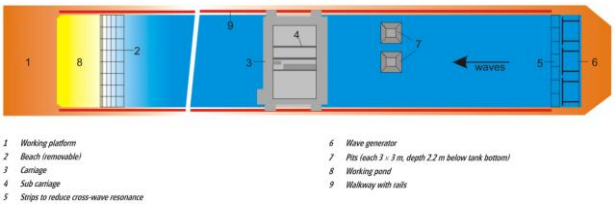

Figure 1: Top view of shallow water basin.

3.2 INSTRUMENTATION,DATA ACQUISITION

In order to measure the wave elevation, a large number of portable electric resistance type wave probes was used. These probes measure the increase of resistance due to the change in wetted part of the wire and based on a careful pre-calibration, this is related to the change in

wave elevation. A potentiometer was used to measure the motions of the wave maker. A sampling frequency of 200Hz (model scale) was used. Prior to sampling, the measured signals were filtered using an analogue anti-aliasing filter.

3.3 SETUP

Two types of experiments were carried out, waves propagating over a flat bottom and waves propagating over a sloped bottom. For the first test, the standard basin setup could be used. For the second test, a temporary concrete sloped floor was built into the basin; the plot below shows the configuration in geoscale 1:50. The depth above the deep part is then 30m, and above the shallow part 15m.

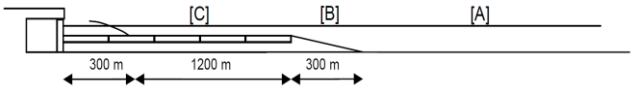

Figure 2: Setup of tests with sloped bottom. A: Deep part. B: slope. C: shallow part.

4. TEST CASES

In this section we illustrate the accuracy of the model and its implementation for four different wave fields, 2 above flat bottom and 2 above a varying bottom that illustrates the change from deep to shallow water in the coastal area.

4.1 FOCUSSING WAVE

The first case is a focussing wave above flat bottom, depth 1m, MARIN experiment 202002. Short, slow, waves are generated before longer, faster, waves, as suggested by Longuet-Higgins [6]. The wave group is designed in such a way that they collide at one point downstream, the focussing point, at which all phases vanish so that all waves contribute to maximize the amplitude. The surface elevation measured at 10m form the wave maker, are used as influx data for the simulations. Although the large crest height is mainly due to the dispersive focussing, close to the focussing point the spectrum broadens due to nonlinear effects; this is well captured by the simulations, just as the wave profile.

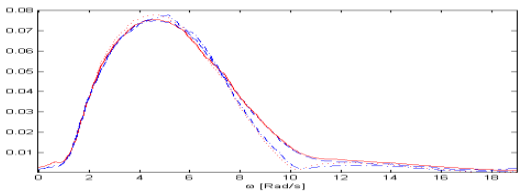

Figure 3: Upper plot: Spectra at 49.5m (blue dashed-dot for experiment, red dot for simulation) and the broadening at 50m (blue dashed for experiment, solid red for simulation).

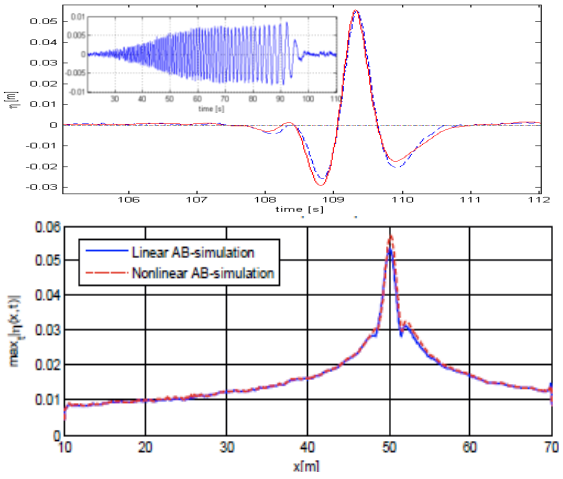

Figure 4: Upper plot: Time signal of the measurement (blue dashed) and of simulation (red solid) at (focussing) position 50m, with the initial elevation at 10m as inset. Lower plot: Showing the focussing phenomenon by the graph of the maximal wave height at each position; blue solid for linear equation and red dashed for the nonlinear model.

4.2 DRAUPNER WAVE

The other case above flat bottom is a short signal (MARIN case 204001) that models the well-known freak wave that was recorded at the Draupner platform in the North Sea at 1 January 1995.

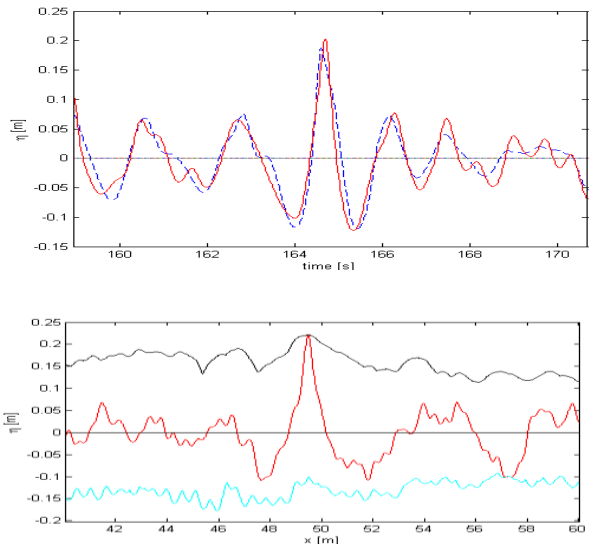

Figure 5: Upper plot: Time signal of the measurement (blue, dashed) at position 40m after the influx position, near the position of maximal crest height, and the signals of simulation (red, solid).
Lower plot: Spatial plot with the maximal (black, upper curve) and minimal (cyan, lower curve) elevation over the full simulation time-interval, and the wave profile (red, solid) at the time of maximal crest height.

4.3 BI-CHROMATIC WAVES

In order to show the interaction of waves with varying bottom, and in particular to investigate the generation of long and short waves, we compare the spectra from simulation with measurements (MARIN case 305002) for a bichromatic wave group. The bathymetry, scaled 1:50 to geophysical dimensions, changes from a depth of 30m to a depth of 15m through a straight 1:20 slope.

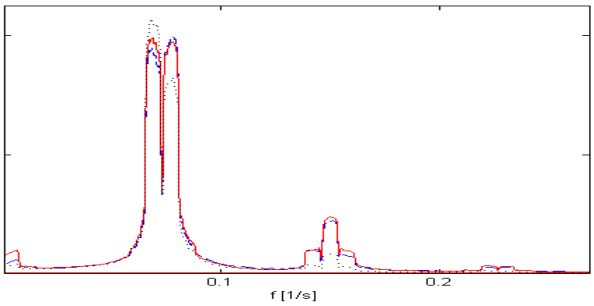

Figure 6: Spectrum of the initial signal above 30m depth (black dot), and of the signal above 15m depth of the simulation (red solid) and measurement (blue dashed). Observe the significant short wave generation of second and third order.

4.4 IRREGULAR WAVES

The last example is a simulation of more than 1000 irregular waves of JONSWAP-type. The bathymetry is the same as in the previous case. In geo-scale, the peak period is 12s, and significant wave height is 3 m (MARIN case 103001).

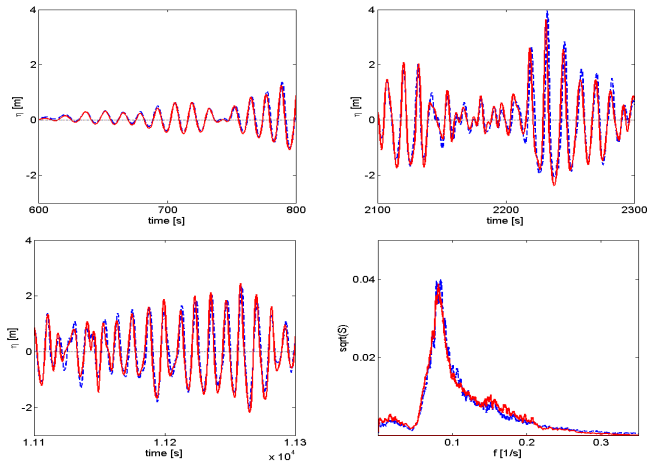

Figure 7: Shown are in three panels time signals of 200s length, and in the fourth panel the spectra computed for the full time trace of 3.5hrs; the measurement (blue, dashed) and simulation (red solid) at a position in the shallow area, 5930 m after the influx position. The results are presented here in geo-scale 1:50 compared to the MARIN-measurement.

5. CONCLUSIONS

The present paper includes a short description of the AB-model and a hybrid spectral-spatial implementation and shows the performance of the code for wave cases that have been measured accurately at MARIN.

Three cases have in common that the spectra are very broad, while the higher order effects in the bi-chromatic wave also require that waves over a long spectral range are modelled correctly. Our experience with the commercial software package MIKE21 BW [9] and with the free software SWASH [10] is that this broad range causes serious problems for these codes because the dispersion is poorly (or not) resolved for short waves (see [8]). The code presented here produces accurate results, and can be used to support the generation of such waves in hydrodynamic laboratories.

The performance has been illustrated graphically above. To quantify the performance, a rather stringent measure is the value of the 'cosine-correlation' between the measurement and the simulation, i.e. the L_2 innerproduct of the normalized signals. For all cases shown above this value is above 0.85.

The calculation (cpu) time for all cases is below 75% of the physical time at the laboratory scale; for simulations on geo-scale in the coastal area of 1:50, this implies that the calculation time is more than a factor 7 shorter. These times are for a code programmed in Matlab, so that simulations with a compiled program will be even faster.

It should be stressed that the present code is only applicable for non-breaking waves, in contrast to the other codes mentioned above, which limits its applicability for other coastal wave applications or for wave run-up and down calculations.

6. ACKNOWLEDGEMENTS

The research in this paper is supported by Royal Netherlands Academy of Arts and Sciences (KNAW) in the scientific collaboration Indonesia-Netherlands, and by Netherlands Organization of Scientific Research, Technology Section STW, project 7216.

7. REFERENCES

1. E. van GROESEN & ANDONOWATI, 'Variational derivation of KdV-type of models for surface water waves', *Physics Letters A* **366** (2007)195-201

2. J.C. LUKE, 'A variational principle for fluid with a free surface'. *J. Fluid Mech.* **27**(1967)395-397

3. V.E. ZAKHAROV, 'Stability of periodic waves of finite amplitude on the surface of a deep fluid'. *J. Appl. Mech.* **2**(1968)190-194

4. L.J.F. BROER, 'On Hamiltonian theory of surface waves'. *Appl. Sci. Res.* **29** (1974) 430-446

5. J.W. MILES, 'On Hamiltonian's principle for surface waves'. *J. Fluid Mech.* **83**(1977) 153-158

6. M.S. LONGUET-HIGGINS, 'Breaking waves in deep and shallow water', *Proc. 10th Symp.Nav.Hydrodyn*, 1974, pp 597-605

7. E. van GROESEN & ANDONOWATI, 'Fully dispersive dynamic models for surface water waves above varying bottom, Part 1: Model equations', *Wave Motion* **48** (2011) 657-666

8. E. van GROESEN & I. van der KROON, 'Fully dispersive dynamic models for surface water waves above varying bottom, Part 2: Hybrid spatial-spectral implementations', in press *Wave Motion*

9. MIKE 21 BW, http://mikebydhi.com/

10. M. ZIJLEMA, G.STELLING & P. SMIT, 'SWASH: an operational public domain code for simulating wave fields and rapidly varied flows in coastal waters', *Coastal Eng.*, **58** (2011) 992-1012

8. AUTHORS' BIOGRAPHIES

Brenny van Groesen holds a position as full professor in Applied Mathematics at the University of Twente, Netherlands, and acts as Scientific Director of the independent research institute LabMath-Indonesia.
Tim Bunnik is senior researcher at MARIN.
Andonowati is associate professor at ITB, Bandung Institute of Technology, Bandung RI, and is Director of LabMath-Indonesia, Bandung RI.